NASA TECHNICAL NOTE

NASA TN D-7223

NASA TN D-7223

DOUBLE ELECTROSTATIC PROBE FOR MEASURING DENSITY, TEMPERATURE, AND VELOCITY OF A FLOWING PLASMA

by Donald L. Chubb

Lewis Research Center
Cleveland, Ohio 44135

NATIONAL AERONAUTICS AND SPACE ADMINISTRATION • WASHINGTON, D. C. • MARCH 1973

1. Report No.	2. Government Accession No.	3. Recipient's Catalog No.
NASA TN D-7223		

4. Title and Subtitle	5. Report Date
DOUBLE ELECTROSTATIC PROBE FOR MEASURING DENSITY, TEMPERATURE, AND VELOCITY OF A FLOWING PLASMA	March 1973
	6. Performing Organization Code

7. Author(s)	8. Performing Organization Report No.
Donald L. Chubb	E-7281
	10. Work Unit No.
	503-10

9. Performing Organization Name and Address	11. Contract or Grant No.
Lewis Research Center National Aeronautics and Space Administration Cleveland, Ohio 44135	
	13. Type of Report and Period Covered
12. Sponsoring Agency Name and Address	Technical Note
National Aeronautics and Space Administration Washington, D.C. 20546	14. Sponsoring Agency Code

15. Supplementary Notes

16. Abstract

A method for obtaining plasma electron temperature and density, as well as the Mach number and flow velocity from the current-voltage characteristic of a flat-faced double probe, is presented. Calculated momentum fluxes of a flowing argon plasma obtained with this probe are compared with experimentally determined momentum fluxes. Reasonable agreement is obtained.

17. Key Words (Suggested by Author(s))	18. Distribution Statement
Plasma; Probe; Electrostatic; Flow; Electron; Temperature; Density; Velocity; Ion; Potential	Unclassified - unlimited

19. Security Classif. (of this report)	20. Security Classif. (of this page)	21. No. of Pages	22. Price*
Unclassified	Unclassified	21	$3.00

* For sale by the National Technical Information Service, Springfield, Virginia 22151

DOUBLE ELECTROSTATIC PROBE FOR MEASURING DENSITY, TEMPERATURE, AND VELOCITY OF A FLOWING PLASMA

by Donald L. Chubb

Lewis Research Center

SUMMARY

A method for obtaining plasma electron temperature and density, as well as the Mach number and flow velocity from the current-voltage characteristic of a flat-faced double probe, is presented. Calculated momentum fluxes of a flowing argon plasma obtained with this probe are compared with experimentally determined momentum fluxes. Reasonable agreement is obtained.

INTRODUCTION

Electrostatic probes have been used to measure plasma properties for many years (ref. 1). Double probes and Langmuir probes are used to measure the electron temperature and plasma number density in stationary plasmas. However, little work has been done in high velocity plasmas. In this study a double probe was used to measure the plasma Mach number and velocity, as well as the electron temperature and plasma number density.

The following section is an analysis of the double probe. The various plasma properties are deduced from the current-voltage characteristic of the double probe. In the last section experimental results obtained with the double probe are presented.

In the analyses it is assumed that the Debye length of the plasma is less than the probe characteristic dimension. Also, all collisional processes and magnetic-field effects are neglected. Therefore, all collisional mean free paths and the cyclotron radii of the electrons and ions must be large compared with the Debye length.

DETERMINATION OF PLASMA PROPERTIES FROM PROBE DATA

Figure 1(a) is a schematic diagram of the double probe being considered. One face

of the probe is alined perpendicular to the plasma flow, and the other face parallel to the flow. If a potential is applied by the power supply arrangement shown in figure 1(a), the probe current-voltage characteristic will look like figure 1(b).

Since the whole probe system is "floating," no net current can flow from the plasma. For the plasmas to be considered, the ions are "cold" compared with the electrons. As a result, the maximum current that can flow in the system will be determined by the ion saturation current for each face rather than the electron saturation current. Since the ion saturation current is much less than the electron saturation current, the bulk plasma is much less disturbed by a double probe than a probe that collects electron saturation current. Since face 2 is perpendicular to the flow, it will have a larger ion saturation current than face 1. As a result, the maximum positive current I_{2+} is greater than the maximum negative current I_{1+}. In the ideal case I_{2+} and I_{1+} are constant. In reality the sheath about each face continues to grow, thus giving a larger effective current collecting area. As a result the saturation ion currents continue to increase slightly as $|V_d|$ is increased.

If there were no flow velocity ($U = 0$) and both faces of the probe were of equal area, the current-voltage characteristic would be symmetric as shown by the dashed curve in figure 1(b). The case for $U = 0$ is discussed by Chen in reference 1 (p. 178-183).

Now consider how the plasma properties can be deduced from the current-voltage characteristic of the probe. Figure 2 is a schematic diagram of the potential distribution in the plasma between the two faces of the probe. The potentials V_1' and V_2' are measured with respect to ground and V_1 and V_2 with respect to the local plasma potential, $V_{p\ell}$ at each probe face. The difference in plasma potential between face 1 and face 2 is V_c. As a result,

$$V_d = V_1' - V_2' = V_2 - V_1 + V_c \tag{1a}$$

$$V_c = V_{p\ell,1} - V_{p\ell,2} \tag{1b}$$

(Symbols are defined in the appendix.) Since the same current I must flow through both faces of the probe,

$$I = i_{2+} - i_{2-} \tag{2a}$$

$$I = i_{1-} - i_{1+} \tag{2b}$$

where i_{1+} and i_{2+} are the ion currents collected by faces 1 and 2, respectively, and i_{1-} and i_{2-} are the electron currents collected by faces 1 and 2, respectively. (Eq. (2)

assumes that the positive direction for current flow is from face 2 to face 1.)

Also, since the whole probe system is floating, no net current is collected from the plasma, thus

$$i_{1+} + i_{2+} - i_{1-} - i_{2-} = 0 \tag{3}$$

Equation (3) shows that

$$i_{1+} + i_{2+} = i_{1-} + i_{2-} \tag{4}$$

We now assume that, in the sheath surrounding each face, the electron density obeys the Boltzmann density distribution (ref. 1, p. 135). Furthermore, we assume that the densities outside the sheath on each probe face are the same and that the electron temperatures at each face are the same. Thus,

$$n_{1-} = n_\infty e^{-qV_1/kT_e} \tag{5a}$$

$$n_{2-} = n_\infty e^{-qV_2/kT_e} \tag{5b}$$

where n_∞ is the plasma density outside the sheath and T_e is the electron temperature. The electron current collected by each face is, therefore,

$$i_{1-} = A_1 n_{1-} \frac{\bar{v}_e}{4} \tag{6a}$$

$$i_{2-} = A_2 n_{2-} \frac{\bar{v}_e}{4} \tag{6b}$$

where A_1 and A_2 are the probe surface areas and $\bar{v}_e$ is the average electron thermal speed, which may be expressed as

$$\bar{v}_e = \sqrt{\frac{8kT_e}{\pi m_e}} \tag{7}$$

Because we are assuming that the Debye length is small compared with the probe radius, the collection area for current is just the surface area of the probe face.

Using equations (5) and (7) in equation (6) gives

$$i_{1-} = A_1 n_\infty \sqrt{\frac{kT_e}{2\pi m_e}}\, e^{-qV_1/kT_e} \tag{8a}$$

$$i_{2-} = A_2 n_\infty \sqrt{\frac{kT_e}{2\pi m_e}}\, e^{-qV_2/kT_e} \tag{8b}$$

In using equation (8) for the electron current collected by the probe, we have neglected the contribution to i_{2-} from the directed velocity U. However, since

$$U << \sqrt{\frac{kT_e}{m_e}}$$

for most plasmas this is a good assumption.

Now substituting equation (8) into equation (4) yields

$$i_{1+} + i_{2+} = n_\infty \sqrt{\frac{kT_e}{2\pi m_e}} \left(A_1 e^{-qV_1/kT_e} + A_2 e^{-qV_2/kT_e} \right) \tag{9}$$

And dividing equation (9) by equation (8b) using equation (1a) results in

$$\frac{i_{1+} + i_{2+}}{i_{2-}} = \frac{A_1}{A_2} \exp\left(\frac{qV_d}{kT_e} - \frac{qV_c}{kT_e} \right) + 1 \tag{10}$$

Substituting equation (2a) for i_{2-} yields

$$\frac{i_{1+} + i_{2+}}{i_{2+} - I} - 1 = \frac{A_1}{A_2} \exp\left(\frac{qV_d}{kT_e} - \frac{qV_c}{kT_e} \right) \tag{11}$$

This is the expression given by Johnson and Malter (ref. 2).

Taking the logarithm of equation (11) yields

$$\ln\left(\frac{i_{1+} + i_{2+}}{i_{2+} - I} - 1\right) = \ln\frac{A_1}{A_2} - \frac{qV_c}{kT_e} + \frac{qV_d}{kT_e} \tag{12}$$

Equation (12) shows that a plot of the left-hand side as a function of V_d should yield a straight line. The slope of the line is equal to the inverse of the electron temperature in electron volts. In many cases it is assumed that i_{2+} and i_{1+} are constant. However, Johnson and Malter (ref. 2) found that i_{2+} and i_{1+} could be approximated by linear functions of V_d. Making this approximation, equation (12) can be written as

$$\ln\left(\frac{AV_d + B}{a_2V_d + b_2 - I} - 1\right) = c_1 + c_2V_d \tag{13}$$

where

$$i_{1+} = a_1V_d + b_1 \tag{14a}$$

$$i_{2+} = a_2V_d + b_2 \tag{14b}$$

$$A = a_1 + a_2 \tag{15a}$$

$$B = b_1 + b_2 \tag{15b}$$

$$c_1 = \ln\frac{A_1}{A_2} - \frac{qV_c}{kT_e} = \ln\frac{A_1}{A_2} - c_2V_c \tag{16a}$$

$$c_2 = \frac{q}{kT_e} \tag{16b}$$

The constants a_1, b_1, a_2, and b_2 can be obtained by fitting a straight line to the ion saturation regions of the probe trace. Using the experimental data to be presented later, a least squares curve fit (ref. 3) of equation (13) was made to obtain c_1 and c_2. In this case

$$c_1 = \frac{X_2P_1 - X_1P_2}{NX_2 - X_1^2} \tag{17}$$

$$c_2 = \frac{NP_2 - X_1P_1}{NX_2 - X_1^2} \tag{18}$$

where

$$X_1 = \sum_{i=1}^{N} V_{d_i} \tag{19a}$$

$$X_2 = \sum_{i=1}^{N} V_{d_i}^2 \tag{19b}$$

$$P_1 = \sum_{i=1}^{N} \ln\left(\frac{AV_{d_i} + B}{a_2V_{d_i} + b_2 - I_i} - 1\right) \tag{19c}$$

$$P_2 = \sum_{i=1}^{N} V_{d_i} \ln\left(\frac{AV_{d_i} + B}{a_2V_{d_i} + b_2 - I_i} - 1\right) \tag{19d}$$

The quantity N is the total number of data points.

A value for the flow Mach number can be obtained from the ratio of front face saturation ion current to side face saturation ion current. In reference 4, the following result for the saturation ion current to a probe in a plasma moving with velocity U is presented:

$$I_+ = A_{pr}qn_\infty \left(U^2 + \frac{8kT_i}{\pi m_i}\right)^{1/2} \qquad U > 0 \tag{20a}$$

If U = 0, the Bohm expression for saturation ion current (ref. 1, p. 150) replaces equation (20a):

$$I_+ = \frac{1}{2} A_{pr} q n_\infty \sqrt{\frac{kT_e}{m_i}} \qquad U = 0 \tag{20b}$$

where A_{pr} is the probe surface area and m_i is the ion mass. Using equations (20a) and (20b) results in

$$\frac{I_{2+}}{I_{1+}} = 2 \sqrt{\frac{U^2 + \frac{8kT_i}{m_i \pi}}{\frac{kT_e}{m_i}}} \tag{21}$$

Equation (21) assumes that $A_{pr_1} = A_{pr_2}$. In most cases $U^2 >> 8kT_i/\pi m_i$, so that

$$\frac{I_{2+}}{I_{1+}} \approx \frac{2U}{\sqrt{\frac{kT_e}{m_i}}} \tag{22}$$

The definition of Mach number is

$$M_\infty^2 \equiv \frac{\rho_\infty U^2}{\gamma p_\infty} \tag{23}$$

where ρ_∞ is the plasma density, p_∞ is the plasma pressure, and γ is the ratio of specific heats. Since neutrality exists in the plasma,

$$n_i \approx n_e = n_\infty$$

$$\rho_\infty = n_\infty (m_e + m_i) \approx m_i n_\infty \tag{24}$$

$$p_\infty = n_\infty (kT_i + kT_e) \tag{25a}$$

In most cases the ion temperature T_i is much less than the electron temperature T_e. As a result,

$$p_\infty \approx n_\infty k T_e \tag{25b}$$

Now substitute equations (24) and (25b) into equation (23).

$$M_\infty^2 \approx \frac{m_i U^2}{\gamma k T_e} \tag{26}$$

Using equation (22) in equation (26) yields

$$M_\infty = \frac{1}{2\sqrt{\gamma}} \left(\frac{I_{2+}}{I_{1+}} \right) \tag{27}$$

Equation (27) gives the plasma Mach number in terms of the ion saturation currents. It is not necessary to know T_e in order to determine the Mach number. A simple measurement of the saturation ion currents collected by the two faces of the probe is all that is necessary.

With M_∞ and T_e known, the plasma flow velocity U can be calculated from equation (26)

$$U = M_\infty \sqrt{\gamma \frac{k T_e}{m_i}} \tag{28}$$

Also, knowing the saturation ion current I_{1+} and the electron temperature T_e, equation (20b) can be used to find the plasma density n_∞. From (20b), remembering that $U = 0$ for face 1,

$$n_\infty = \frac{2 I_{1+}}{q A_{pr}} \sqrt{\frac{m_i}{k T_e}} \tag{29}$$

Equations (16a) and (27) to (29) enable one to calculate the electron temperature, plasma Mach number, plasma velocity, and plasma number density from the double probe current-voltage characteristic. In the next section these properties will be calculated from an experimental probe trace.

EXPERIMENTAL RESULTS

Construction of the flat-faced double probe used in the experiment is illustrated in figure 3. Also shown is the electrical circuit. Shields were placed around each face of the probe. The shields are biased independently to the same potential as the face they enclose. This was done to reduce the amount of current arriving at a probe face from any direction other than that perpendicular to the probe face. In other words, to make the probe as one-dimensional as possible. The independent biasing of the shields and probe faces is accomplished by mounting matched potentiometers on the same shaft.

The following procedure was used to construct the double probe. A 0.0508-centimeter-diameter tantalum wire was placed inside the 0.203-centimeter-outside-diameter tantalum tube. The space between the wire and tube was then packed with magnesium oxide. To insure a tight fit between the wire and tube, the tantalum tube was then swagged down to an approximately 0.165-centimeter outside-diameter. The resulting tube-wire combination was bent to a 45° angle at one end. The end was then machined at a 45° angle to produce one section of the probe. A similar procedure was carried out with another wire-tube combination to produce the other section of the probe. Each section was then placed in an oval-shaped, two-holed ceramic tube to complete the construction. The area of each face was 2.87×10^{-3} square centimeter.

With a magnetoplasmadynamic (MPD) arc (ref. 5) as the source for a flowing argon plasma, a typical current-voltage characteristic for the double probe is shown in figure 4. The current in the ion saturation regions of the curve increases faster with no bias potential on the shields than it does with bias potential on the shields. Biasing the shields causes the current to be almost constant in the ion saturation regions. This is the expected result for a purely one-dimensional probe. In figure 4 only probe face 1, which is parallel to the flow, shows the effect of a biased shield. However, in other cases the effect has been noted in both ion saturation regions. The probe curve was unchanged outside the ion saturation regions with or without shield biasing. The plasma parameters are determined mainly by the region of the probe curve between the ion saturation regions. Therefore, we conclude that any potential difference that may develop between one of the probe faces and its corresponding shield as a result of the independent biasing of the shields has negligible effect on the plasma parameters deduced from the probe curve.

Probe current-voltage data were sent directly to an IBM 360 computer. Programming equations (16) to (19) and (27) to (29) allowed on-line computation of the electron temperature, plasma Mach number, velocity, and density. The saturation currents, I_{2+} and I_{1+}, were taken at the points where the linear saturation portions of the probe trace (fig. 4) begin to deviate from the exponentially varying middle portion of the trace. Figure 5 compares the experimentally determined left-hand side of equation (13) with the

least squares approximation of this function given by the right-hand side of equation (13). Slightly different results occur depending on the number of data points used in the least squares approximation. Including more points in the ion saturation portion of the current-voltage characteristic produced higher electron temperatures and a poorer fit in the region between the ion saturation portions. Including points for $-6 \leq V_d \leq 12$ yielded $kT_e/q = 2.01$ electron volts, and points for $-2.5 \leq V_d \leq 7.5$ yielded $kT_e/q = 1.80$ electron volts. Table I summarizes the results obtained from the data given in figure 4.

To check the double probe results, a comparison was made between the momentum flux, $m_i n_\infty U^2$, calculated from double probe results, and the momentum flux, determined by measuring the thrust of the MPD arc. Because the Mach number of the flow is high, the pressure term is small when compared with the momentum flux term in the equation of motion. Therefore, the thrust produced by the MPD arc is just the integrated momentum flux in the beam:

$$T = \int_{A_b} m_i n v^2 dA_b + \int_{A_b} m_o n_o v_o^2 dA_b \tag{30}$$

The first integral is the thrust contribution from the ions, and the second integral the contribution from the neutrals. Since the electron mass is small, the electron momentum has been neglected in equation (30). Terms appearing in equation (30) are the ion mass m_i, the electron density n, the ion velocity v, the neutral mass m_o, the neutral density n_o, the neutral velocity v_o, and the plasma beam cross sectional area A_b. In using the electron density in equation (30) we are assuming charge neutrality.

If we assume that the density and velocity are independent of azimuthal angle and that $m_i \approx m_o$, then equation (30) becomes

$$T = 2\pi m_i \int_0^R n v^2 r \, dr + 2\pi m_i \int_0^R n_o v_o^2 r \, dr \tag{31}$$

where R is the radius of the plasma beam. In order to carry out the integrations in equation (31), the radial dependence of the densities and velocities must be known. The double probe can be used to determine the ion velocity and density distributions. However, there is no convenient way to obtain the neutral density and velocity distributions. As a result, we approximated the neutral thrust contribution as follows:

$$T_o = 2\pi m_i \int_0^R n_o v_o^2 r \, dr \approx \dot{m}_o U_o \tag{32}$$

where $\dot{m}_o$ is the neutral mass flow rate and U_o is some average neutral velocity.

Using equation (32) in (31) yields the following:

$$T = 2\pi m_i \int_0^R nv^2 r \, dr + \dot{m}_o U_o \tag{33}$$

The neutral flow rate can be obtained from the measured total mass flow rate $\dot{m}_t$ and the calculated ion flow rate $\dot{m}_i$:

$$\dot{m}_o = \dot{m}_t - \dot{m}_i = \dot{m}_t - 2\pi m_i \int_0^R nvr \, dr \tag{34}$$

Substituting equation (34) into (33) yields

$$T = 2\pi m_i \int_0^R nv^2 r \, dr + U_o\left[\dot{m}_t - 2\pi m_i \int_0^R nvr \, dr\right] \tag{35}$$

Double probe data for the density and velocity distributions at an axial station 61 centimeters from the exit of the MPD arc is shown in figures 6 and 7. We approximated these data with the following functions:

$$n = n_\infty e^{-ar} \tag{36}$$

$$v = U\left(1 - \frac{r}{R}\right) \tag{37}$$

where n_∞ and U are the density and velocity in the center of the beam. Fitting the data in figures 6 and 7 with the straight lines shown, we find that $R \approx 40.7$ centimeters and $1/a \approx 6.27$ centimeters.

Substituting equations (36) and (37) into (35) yields the following result:

$$T = \frac{2\pi m_i n_\infty U^2}{a^2}\left[\left(1 - \frac{4}{aR} + \frac{6}{a^2R^2}\right) - \frac{2e^{-aR}}{aR}\left(1 + \frac{3}{aR}\right)\right] + U_o\left[\dot{m}_t - \frac{2\pi m_i n_\infty U}{a^2}\left(1 - e^{-aR}\right)\right] \tag{38}$$

For argon with $1/a = 6.27$ centimeters and $R = 40.7$ centimeters, equation (38) becomes

$$T = 8.53\times10^{-28}\, n_\infty U^2 + U_0(\dot{m}_t - 1.64\times10^{-27}\, n_\infty U) \quad \text{(SI units)} \tag{39}$$

The ion velocity U and density n_∞ are obtained from the double probe results. However, we have no measurement of the neutral average velocity U_0. Certainly $U_0 \leq U$, since the neutrals are accelerated by collisions with the ions. Sovie and Connolly (ref. 6) measured ion and neutral velocities in the exhaust of an MPD arc running on ammonia. Based on their results, we approximated the average neutral velocity as $U_0 \approx 2/3\ U$. Using $U_0 = 2/3\ U$ as well as the velocities and densities given in table I in equation (39) yields the results for thrust shown in tableII. The experimentally determined thrust was 0.28 newton.

A comparison of the calculated and measured thrusts shows that there is reasonable agreement between them. The calculated thrust is about 30 percent less than the measured thrust. If we assume that $U_0 \approx U$ then the measured and calculated thrusts are almost equal. Therefore, within the accuracy of the neutral thrust approximation, we conclude that the plasma properties determined by the double probe are a good approximation to actual plasma properties.

CONCLUSIONS

A method is presented for calculating the plasma electron temperature, number density, flow Mach number, and flow velocity based on the current-voltage characteristic of a flat-faced double probe. The analysis assumes a Maxwellian distribution function for the electrons. Experimental results for the plasma properties using a double probe were obtained in the exhaust of an magnetoplasmadynamic (MPD) arc. The thrust calculated using the double probe determined plasma properties was compared with the measured thrust. Reasonable agreement was found, indicating that the double-probe determined plasma properties are a good approximation to the actual plasma properties.

Lewis Research Center,
National Aeronautics and Space Administration,
Cleveland, Ohio, January 17, 1973,
503-10.

APPENDIX - SYMBOLS

A	constant defined by eq. (15a)
A_b	cross sectional area of MPD arc beam
A_{pr}	probe surface area
A_s	sheath area
A_1	surface area of face 1 of double probe
A_2	surface area of face 1 of double probe
B	constant defined by eq. (15b)
c_1	constant defined by eqs. (16a) and (17)
c_2	constant defined by eqs. (16b) and (18)
I	probe current
I_{1+}	saturation ion current to probe face 1
I_{2+}	saturation ion current to probe face 2
i_{1+}	ion current to probe face 1
i_{2+}	ion current to probe face 2
i_{1-}	electron current to probe face 1
i_{2-}	electron current to probe face 2
i_-	electron current to Langmuir probe
i_+	ion current to Langmuir probe
k	Boltzmann constant (1.38×10^{-23} J/K)
M_∞	Mach number outside probe sheath
m	mass
$\dot{m}$	mass flow rate
n_1	electron number density in sheath about probe face 1
n_2	electron number density in sheath about probe face 2
n_∞	electron number density outside probe sheath
P_1	defined by eq. (19c)
P_2	defined by eq. (19d)
p	pressure

q	magnitude of electron charge (1.602 C)
r	radius in cylindrical coordinate system
T	total thrust
T_{cal}	total calculated thrust
T_e	electron temperature
T_o	neutral thrust
U	velocity of ion flow
U_o	velocity of neutral flow
V	electric potential
V_c	difference in plasma potential between probe face 1 and face 2
V_d	difference in potential between probe face 2 and face 1 of double probe
V_{pl}	plasma potential
V_1	potential of probe face 1 with respect to plasma potential
V_2	potential of probe face 2 with respect to plasma potential
V_1'	potential of probe face 1 with respect to ground potential
V_2'	potential of probe face 2 with respect to ground potential
v	velocity
$\bar{v}_e$	average electron thermal speed
X_1	defined by eq. (19a)
X_2	defined by eq. (19b)
γ	ratio of specific heats
ϵ_o	permittivity of free space (8.855×10^{-12} F/m)

REFERENCES

1. Chen, Francis F.: Electric Probes. Plasma Diagnostic Techniques. R. H. Huddlestone and S. L. Leonard, eds., Academic Press, 1965, pp. 113-200.

2. Johnson, E. O.; and Malter, L.: A Floating Double Probe Method for Measurements in Gas Discharges. Phys. Rev., vol. 80, no. 1, Oct. 1, 1950, pp. 58-68.

3. Sokolnikoff, I. S.; and Redheffer, R. M.: Mathematics of Physics and Modern Engineering. McGraw-Hill Book Co., Inc., 1958, pp. 702-704.

4. Fahleson, U.: Theory of Electric Field Measurements Conducted in the Magnetosphere with Electric Probes. Space Sci. Rev., vol. 7, 1967, pp. 238-262.

5. Seikel, George R.; Connolly, Denis J.; Michels, Charles J.; Richley, Edward A.; Smith, J. Marlin; and Sovie, Ronald J.: Plasma Physics of Electric Rockets. Plasmas and Magnetic Fields in Propulsion and Power Research. NASA SP-226, 1970, pp. 1-64.

6. Sovie, R. J.; and Connolly, D. J.: A Study of the Axial Velocities in an Ammonia MPD Thruster. AIAA J., vol. 7, no. 4, Apr. 1969, pp. 723-725.

TABLE I. - COMPARISON OF PLASMA PROPERTIES DETERMINED FROM DOUBLE-PROBE CURRENT-VOLTAGE CHARACTERISTICS

[Data obtained from fig. 4.]

Range of data points considered, V	Saturation ion current, mA		Electron temperature, T_e, eV	Mach number, M_∞	Ion flow velocity, U, m/sec	Number density, n_∞, m^{-3}
	I_{1+}	I_{2+}				
$-6 \leq V_d \leq 12$	0.040	0.490	2.01	4.72	1.34×10^4	7.99×10^{17}
$-2.5 \leq V_d \leq 7.5$	.040	.490	1.80	4.72	1.27×10^4	8.42×10^{17}

TABLE II. - COMPARISON OF THRUST CALCULATED FROM DOUBLE PROBE RESULTS AND MEASURED THRUST

[Ion mass flow rate, 1.76×10^{-5} kg/sec; neutral mass flow rate, 9×10^{-6} kg/sec; total mass flow rate, 2.66 kg/sec; measured thrust, 0.28 N.]

Number density, n_∞, m^{-3}	Ion velocity, U, m/sec	Neutral velocity, $U_o = \frac{2}{3} U$	Ion thrust, T_i, N	Neutral thrust, T_o, N	Total thrust, $T_{cal} = T_i + T_o$, N
7.99×10^{17}	1.34×10^4	8.94×10^3	0.122	0.081	0.203
8.42	1.27	8.47	.115	.076	.191

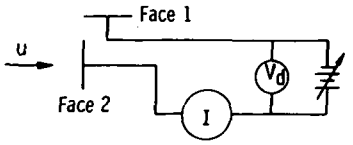

(a) Schematic diagram.

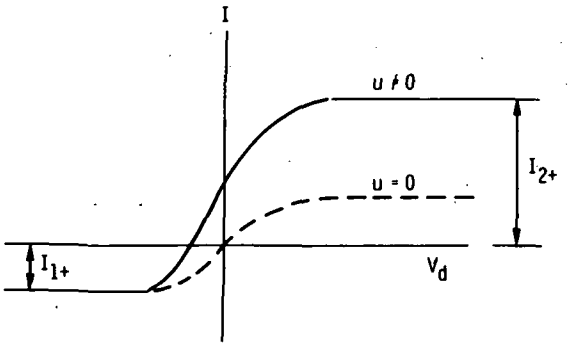

(b) Ideal current-voltage characteristic.

Figure 1. - Double velocity probe.

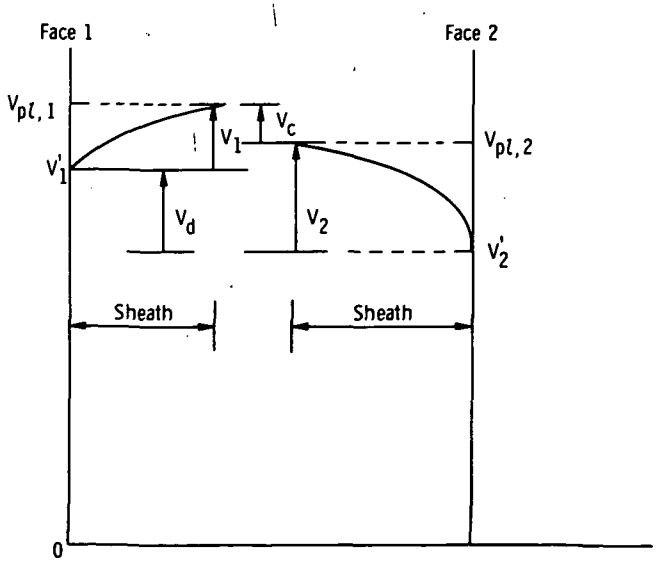

Figure 2. - Potential distribution between double probe faces.

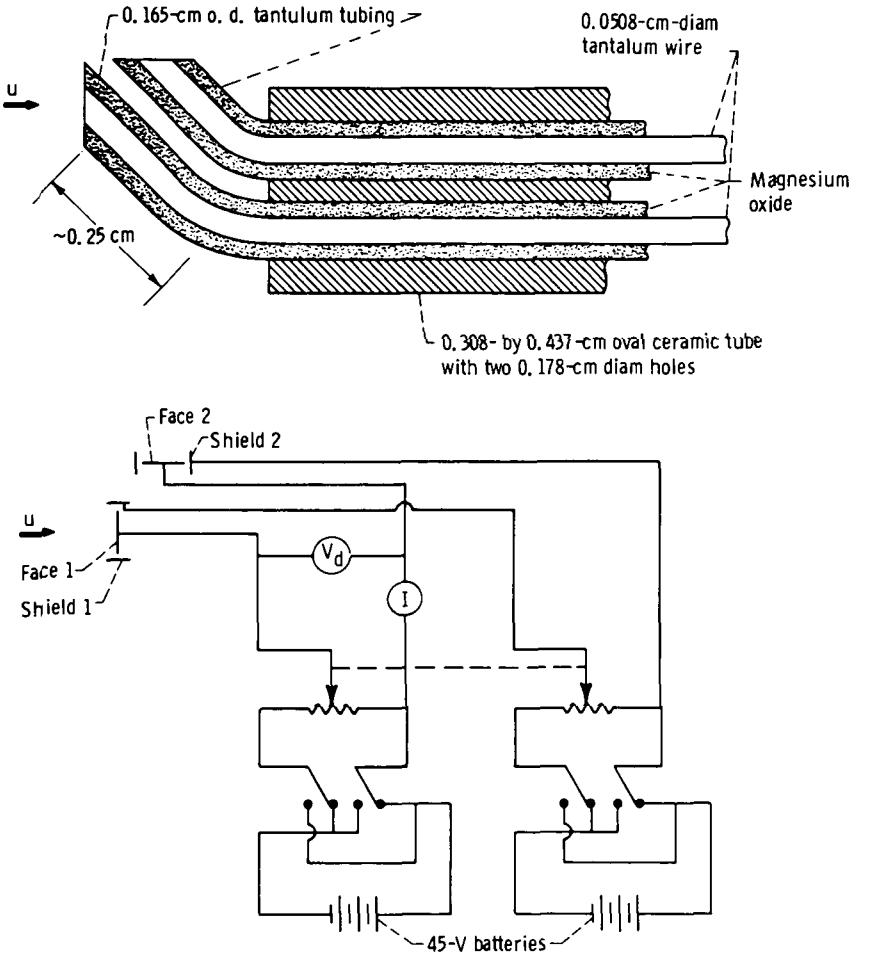

Figure 3. - Double velocity probe construction.

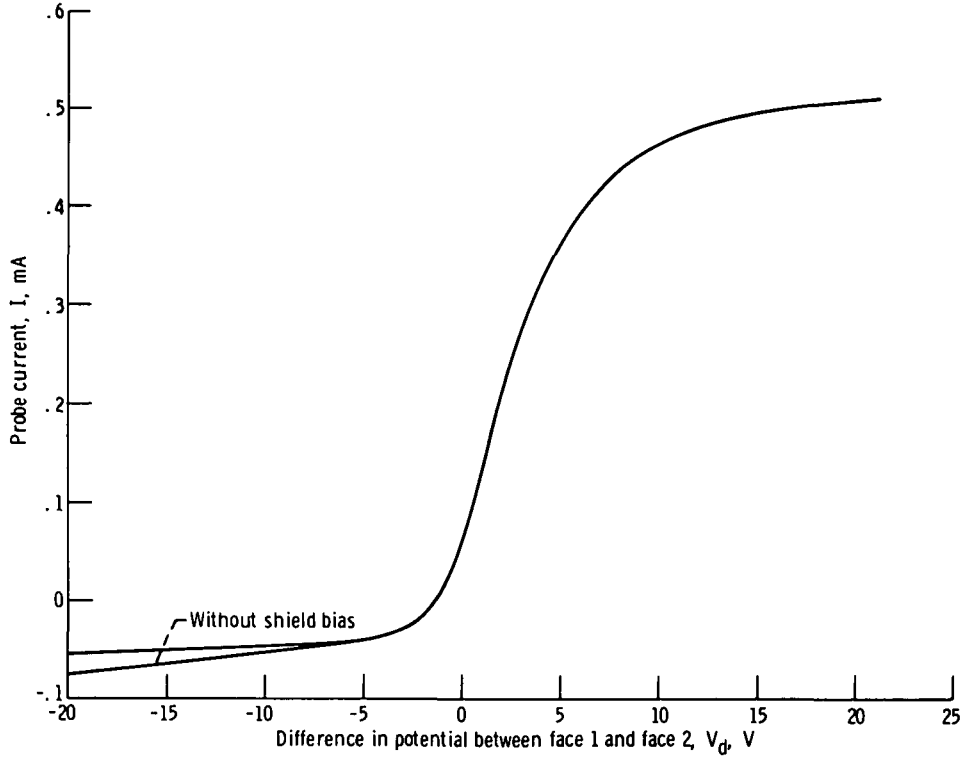

Figure 4. - Typical current-voltage characteristic of double velocity probe in argon.

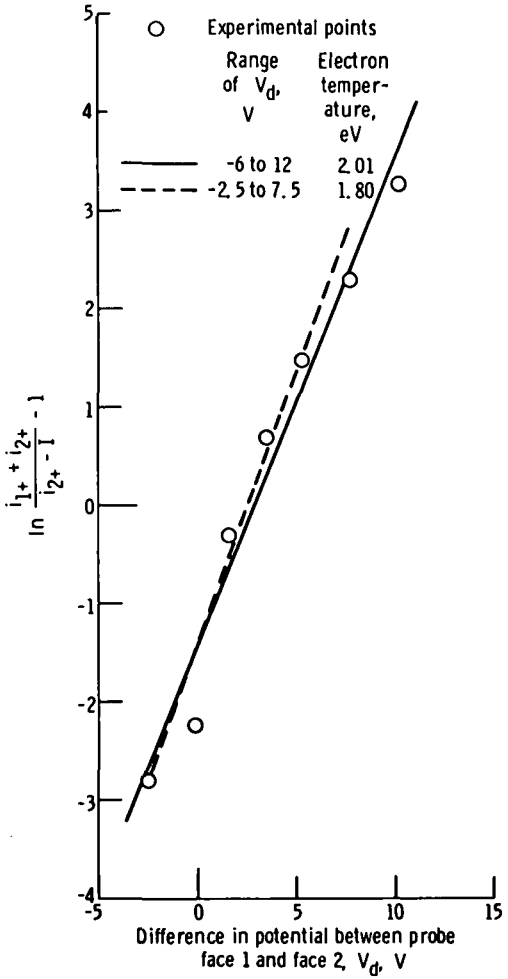

Figure 5. - Comparison of experimental data and calculated electron temperatures. (Data from fig. 4.)

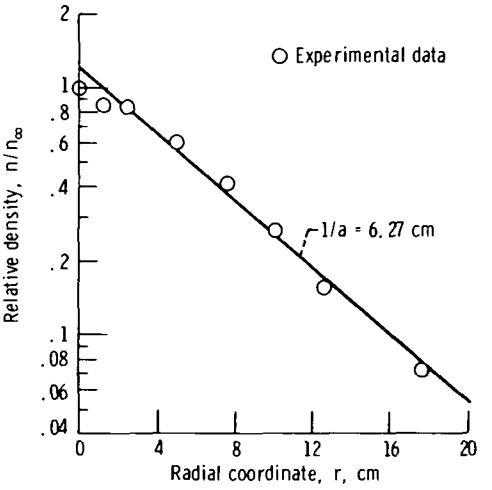

Figure 6. - Radial density profile in magneto-plasmadynamic arc. ($n/n_\infty = e^{-ar}$.)

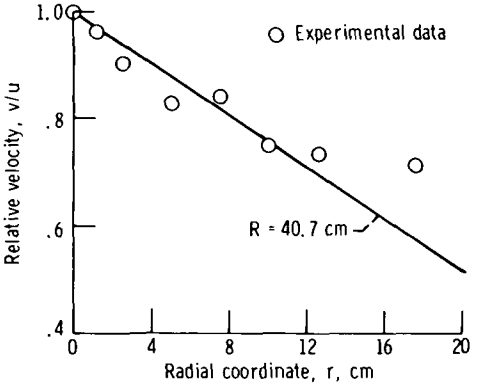

Figure 7. - Radial velocity profile in magneto-plasmadynamic arc. $\left(\frac{v}{u} = 1 - \frac{r}{R}\right)$

NASA-Langley, 1973 — 25 E-7281

NATIONAL AERONAUTICS AND SPACE ADMINISTRATION
WASHINGTON, D.C. 20546

OFFICIAL BUSINESS
PENALTY FOR PRIVATE USE $300

SPECIAL FOURTH-CLASS RATE
BOOK

POSTAGE AND FEES PAID
NATIONAL AERONAUTICS AND
SPACE ADMINISTRATION
451

U.S.MAIL

POSTMASTER : If Undeliverable (Section 158 Postal Manual) Do Not Return

"The aeronautical and space activities of the United States shall be conducted so as to contribute . . . to the expansion of human knowledge of phenomena in the atmosphere and space. The Administration shall provide for the widest practicable and appropriate dissemination of information concerning its activities and the results thereof."

—NATIONAL AERONAUTICS AND SPACE ACT OF 1958

NASA SCIENTIFIC AND TECHNICAL PUBLICATIONS

TECHNICAL REPORTS: Scientific and technical information considered important, complete, and a lasting contribution to existing knowledge.

TECHNICAL NOTES: Information less broad in scope but nevertheless of importance as a contribution to existing knowledge.

TECHNICAL MEMORANDUMS: Information receiving limited distribution because of preliminary data, security classification, or other reasons. Also includes conference proceedings with either limited or unlimited distribution.

CONTRACTOR REPORTS: Scientific and technical information generated under a NASA contract or grant and considered an important contribution to existing knowledge.

TECHNICAL TRANSLATIONS: Information published in a foreign language considered to merit NASA distribution in English.

SPECIAL PUBLICATIONS: Information derived from or of value to NASA activities. Publications include final reports of major projects, monographs, data compilations, handbooks, sourcebooks, and special bibliographies.

TECHNOLOGY UTILIZATION PUBLICATIONS: Information on technology used by NASA that may be of particular interest in commercial and other non-aerospace applications. Publications include Tech Briefs, Technology Utilization Reports and Technology Surveys.

Details on the availability of these publications may be obtained from:

SCIENTIFIC AND TECHNICAL INFORMATION OFFICE

NATIONAL AERONAUTICS AND SPACE ADMINISTRATION

Washington, D.C. 20546